

PECULIARITIES OF THE NONEQUILIBRIUM DISTRIBUTION OF MOISTURE  
IN THE FREEZING AND THAWING OF DISPERSE SOILS

Yu. S. Danielyan and P. A. Yanitskii

UDC 536.421

The article presents the results of numerical simulation of the process of moisture migration in disperse soils with different regimes of freezing and with a view to the nonequilibrium effects accompanying the phase transformations of water. The results of simulation are compared with data of experimental investigations from the literature.

Among the problem of heat and mass exchange in freezing and thawing soils, the investigation of the dynamics of moisture redistribution takes up a special place. At present there exists a number of publications containing the results of experimental investigations of moisture migration in different freezing regimes. The authors of [1, 2] describe experiments with the one-sided freezing of moist soil samples; the redistribution of moisture in a sample of frozen soil affected by a constant temperature gradient is investigated in [3]. There are much fewer theoretical works [4, 5] in which such problems are solved. This is possibly due to the insufficient utilization of simulation, i.e., the theoretical solution of problems of heat and mass exchange whose mathematical statement contains the notions of simulating various physical effects and processes accompanying the freezing and thawing of disperse materials; the authors of [6, 7] present the results of theoretical and experimental investigations of nonequilibrium crystallization during the freezing of moist soils without taking moisture migration into account. The model of crystallization of moisture in the soil under isothermal conditions is described in [6].

Principal System of Equations. In the one-dimensional case, the system of equations describing the nonequilibrium heat and mass exchange during the freezing (thawing) of soils has the following form:

$$c(W, T, L) \frac{\partial T}{\partial t} = \frac{\partial}{\partial x} \left( \lambda(W, T, L) \frac{\partial T}{\partial x} \right) - \alpha \frac{\partial L}{\partial t}, \quad (1)$$

$$\frac{\partial W_s}{\partial t} = \frac{\partial q}{\partial x}, \quad W_s = W + L, \quad (2)$$

$$\frac{\partial L}{\partial t} = \alpha(W - W_{of}(T)), \quad (3)$$

where

$$\alpha = \sigma(T_{of}(W) - T) \frac{1}{\tau_{cr}} + \sigma[(T - T_{of}(W))L] \frac{1}{\tau_{me}} \quad (4)$$

Equations (1) and (2) of this system are the mathematically expressed laws of conservation of energy and mass; the third equation describes the kinetics of the phase transitions of water [6]. To close the system (1)-(4) it must be complemented by the hypothesis of migration. In the given system the migration stream  $q$  is determined by the simulation ratio  $q = k(W - \underline{W})\partial W/\partial x$ , where  $\underline{W}$  is some limiting moisture below which moisture transport in the liquid phase ceases. In addition to that, it is assumed here that the magnitude of the migration stream is determined by the same ratio both in the thawed and in the frozen zones. It should be pointed out that to this day there does not exist any acceptable method of measuring moisture transport in the frozen zone; therefore, the experimental data given in various works do not make it possible to present a sufficiently substantiated hypothesis

V. I. Muravlenko State Research and Project Institute of the Petroleum and Gas Industry, Tyumen'. Translated from *Inzhenerno-Fizicheskii Zhurnal*, Vol. 44, No. 1, pp. 91-98, January, 1983. Original article submitted April 6, 1981.

regarding the regularities of moisture migration at temperatures below zero. The authors of [3], based solely on their own experiments, arrived meanwhile at the conclusion that the expressions for the stream of moisture in the thawed and frozen zones do not differ much from each other. It is especially for this reason that in the present article we adopted a single hypothesis of migration for both zones.

The coefficient  $\alpha$  in (3) and (4) changes in dependence on the direction of the nonequilibrium phase transition (the kinetic model of the thawing of ice was chosen the same as in crystallization). The purpose of writing this coefficient in Eq. (4) is to express the peculiarities of operation of the kinetic equation (3) in the following three different cases:

$$1) T < T_{of}(W), \alpha = \frac{1}{\tau_{cr}}, \frac{\partial L}{\partial t} = \frac{1}{\tau_{cr}} (W - W_{of}(T)) > 0. \text{ Under these conditions } \Delta W = W - W_{of}(T) > 0, \text{ i.e., part of the moisture } \Delta W \text{ is in a nonequilibrium state, and it crystallizes;}$$

$$2) T > T_{of}(W), L > 0, \alpha = \frac{1}{\tau_{me}}, \frac{\partial L}{\partial t} = \frac{1}{\tau_{me}} (W - W_{of}(T)) < 0, \Delta W < 0, \text{ i.e., the nonequilibrium amount of nonfrozen water is smaller than the equilibrium amount } W_{of}(T). \text{ Since here in an elementary volume there is ice } (L > 0), \text{ it thaws;}$$

$$3) T > T_{of}(W), L = 0, \alpha = 0, \frac{\partial L}{\partial t} = 0. \text{ This case corresponds to the thawed zone.}$$

The system (1)-(4) describes heat transfer, moisture transport in the thawed and frozen zones, the phase transition in the spectrum of below-zero temperatures, and the kinetic (relaxation) effects of crystallization of the moisture and of the pressure of the ice. If we neglect the kinetic effects in the phase transitions of the moisture, and also its migration, then the system (1)-(4) describes the problem of freezing (thawing), taking into account the phase transition in the temperature spectrum [8]. Furthermore, in the case of a jumplike change of the amount of nonfreezing water  $W_{of}(T)$  at the temperature of the phase transition  $T = T_{of}$ , it can be shown that the system (1)-(3) corresponds to the known frontal statement of Stefan's problem (see, e.g., [9]). When concrete problems are solved, the system (1)-(4) must be complemented with boundary and initial conditions for the functions of  $T$ ,  $W$ , and  $L$ . A peculiarity of the given statement is that Eqs. (1)-(4) describe heat and mass exchange in both the thawed and frozen zones, and then there is no necessity of specifying additional conditions at the mobile phase interface.

Mathematical Statement of the Problems. It is known that heat capacity and thermal conductivity depend on the temperature, the moisture, and icing up of the soil; however, the nature of these dependences has not yet been sufficiently studied, and therefore these characteristics will henceforth be considered constant and equal in magnitude in the thawed and frozen zones. All these simplifications of the initial problem may be considered justified as long as qualitative investigations and the description of experimental data are involved. A more accurate comparison of the theoretical analysis with experiments should, if possible, be carried out without such simplifications.

For further numerical analysis, it is expedient to represent the system (1)-(4) in dimensionless form:

$$\begin{aligned} \frac{\partial \theta}{\partial Fo} &= \frac{\partial^2 \theta}{\partial \xi^2} + K_0 \frac{\partial l}{\partial Fo}, \\ \frac{\partial \omega}{\partial Fo} + \frac{\partial l}{\partial Fo} &= p \frac{\partial}{\partial \xi} ((\omega - \underline{\omega}) \frac{\partial \omega}{\partial \xi}), \\ \frac{\partial l}{\partial Fo} &= \beta (\omega - \omega_{of}(\theta)). \end{aligned} \quad (5)$$

Here  $\beta = \sigma(\theta_{of}(\omega) - \theta)B_{cr} + \sigma[(\theta - \theta_{of}(\omega))L]B_{me}$ .

In those problems where the investigated soil, on the whole, is in the frozen state, and on its boundaries the temperature remains constant in time, the system (5) may be simplified. For that we will examine the characteristic times of the transient processes of heat and mass transfer, which in the basis of the dimension theory are determined from the ratios  $t_1 = L^2 c/\lambda$ ,  $t_2 = L^2/k W_0$ . With the approximate values of the constants  $c$ ,  $\lambda$ ,  $k$ , and  $W_0$

given in the literature, we can obtain the following inequality:  $t_1 \ll t_2$ . That means that the time of the transient process connected with moisture migration is much longer than the "thermal" time. Consequently, when we analyze the dynamics of moisture redistribution in frozen soils, we may consider the temperature field to be steady. In view of this, system (5) may be written in abbreviated form for such problems:

$$\frac{\partial \omega}{\partial t'} + \frac{\partial l}{\partial t'} = \frac{\partial}{\partial \xi} \left( (\omega - \underline{\omega}) \frac{\partial \omega}{\partial \xi} \right), \quad (6)$$

$$\frac{\partial l}{\partial t'} = D(\omega - \omega_{of}(\theta_{st})).$$

Here  $D = \sigma(\theta_{of}(\omega) - \theta)D_{cr} + \sigma[(\theta - \theta_{of}(\omega))L]D_{me}$ ;  $\theta_{st} = \theta_{st}(\xi)$  is the steady-state temperature distribution. All further investigations are based on the numerical solution of systems (5) and (6), with these or other boundary and initial conditions expressing different freezing and thawing regimes.

Below we examine two problems: one-sided freezing of moist soil, and the redistribution of moisture in a frozen sample under the effect of a constant temperature gradient. The former simulates the heat and mass exchange in a seasonally freezing (thawing) layer, the latter may be used for analyzing the processes of moisture redistribution in permafrost rock masses. These problems are described by the systems of differential equations (5) and (6), respectively, with certain boundary and initial conditions.

In simulating one-sided freezing, the following initial and boundary conditions are adopted:

$$\theta(\xi, 0) = \theta_0, \quad \omega(\xi, 0) = 1, \quad l(\xi, 0), \quad (7)$$

$$\theta(0, Fo) = -1, \quad \theta(1, Fo) = \theta_0, \quad (8)$$

$$\frac{\partial \omega}{\partial \xi}(0, Fo) = 0, \quad \frac{\partial \omega}{\partial \xi}(1, Fo) = 0. \quad (9)$$

Expressions (9) express freezing under conditions of a closed system.

The solution of the problem of moisture redistribution in a frozen sample is given for the following initial and boundary conditions:

$$\omega(\xi, 0) = \omega_{of}(\theta_{st}), \quad l(\xi, 0) = 1 - \omega_{of}(\theta_{st}), \quad (10)$$

$$\frac{\partial \omega}{\partial \xi}(0, \bar{t}) = 0, \quad \frac{\partial \omega}{\partial \xi}(1, \bar{t}) = 0. \quad (11)$$

Here, like with one-sided freezing, it is assumed that the soil is completely moisture insulated. The steady-state temperature distribution is assumed to be linear, and on the boundaries of the examined sample constant values of the dimensionless temperature  $\theta_{st}(0) = 1$ ,  $\theta_{st}(1) = \theta_0$  are specified.

Numerical Simulation. On the axes we plot a uniform grid  $\xi_i = ih$  with time step  $\Delta Fo$ . In the calculations we used an implicit difference scheme, linear relative to the values of the functions  $\theta$ ,  $\omega$  on the upper time layer. The values of the coefficients  $B(\omega - \omega_{of}(\theta))$  and  $\omega - \underline{\omega}$  were calculated from the values of temperature and moisture on the preceding time layer. In finite differences, Eqs. (5) have the form

$$\frac{\theta_i^{n+1} - \theta_i^n}{\Delta Fo} = \frac{1}{h^2} (\theta_{i+1}^{n+1} - 2\theta_i^{n+1} + \theta_{i-1}^{n+1}) + K_{ob} (\omega_i^n - \omega_{of}(\theta_i^n)),$$

$$\frac{\omega_i^{n+1} - \omega_i^n}{\Delta Fo} + B(\omega_i^n - \omega_{of}(\theta_i^n)) = p \frac{1}{h^2} ((\omega_{i+\frac{1}{2}}^n - \underline{\omega})(\omega_{i+1}^{n+1} - \omega_i^{n+1}) - (\omega_{i-\frac{1}{2}}^n - \underline{\omega})(\omega_i^{n+1} - \omega_{i-1}^{n+1})),$$

$$\frac{l_i^{n+1} - l_i^n}{\Delta Fo} = B(\omega_i^n - \omega_{of}(\theta_i^n)),$$

$$B = \sigma(\theta_{of}(\omega_i^n) - \theta_i^n) B_{cr} + \sigma[(\theta_i^n - \theta_{of}(\omega_i^n)) l_i^n] B_{me}.$$

The error of the approximation of the scheme used is  $O(h^2 + \Delta Fo)$ . The coefficient B changes in dependence on the direction of the phase transition crystal-liquid. When  $S = \omega - \omega_{of}(\theta) > 0$ , the moisture crystallizes, and then  $B = B_{cr}$ . When the condition  $S < 0$  is fulfilled and when there is ice at the examined point ( $l > 0$ ), then thawing occurs, i.e.,  $B = B_{me}$ .

To calculate the heat and moisture balance, we must integrate the first two equations of systems (5) with respect to  $\xi$  from 0 to 1 and with respect to Fo from 0 to the running value:

$$\int_0^1 \theta a d\xi \Big|_0^{Fo} = \int_0^{Fo} \frac{\partial \theta}{\partial \xi} dFo \Big|_0^1 + Ko \int_0^1 l a d\xi \Big|_0^{Fo},$$

$$\int_0^1 (\omega + l) a d\xi \Big|_0^{Fo} = p \int_0^{Fo} (\omega - \underline{\omega}) \frac{\partial \omega}{\partial \xi} dFo \Big|_0^1.$$

In accordance with (9), this relation is reduced to the form

$$\int_0^1 \omega_S d\xi \Big|_0^{Fo} = 0, \quad \omega_S = \omega + l.$$

In the count, the following values were calculated:

$$\delta Q_1 = \int_0^1 \bar{\theta} d\xi \Big|_0^{Fo} - \int_0^{Fo} \frac{\partial \bar{\theta}}{\partial \xi} dFo \Big|_0^1 - Ko \int_0^1 \bar{l} a d\xi \Big|_0^{Fo},$$

$$\delta Q_2 = \int_0^1 \bar{\omega}_S d\xi \Big|_0^{Fo}.$$

These values, called the disbalances, characterize the degree of deviation of the numerical solution from the accurate solution in the integral sense. In all the calculations the values of h and  $\Delta Fo$  were chosen in such a way that  $\delta Q_1$  and  $\delta Q_2$  did not exceed 1%. The difference scheme for system (6) is written analogously. The space and time steps are chosen in accordance with the magnitude of the disbalance in the same way as in the previous case.

One-Sided Freezing. The calculations were carried out for kaolinite clay, whose dimensionless equilibrium curve of nonfrozen water is expressed by the ratio  $\omega_{of}(\theta) = 0.2/(0.1 - \theta)$ . The values of the other constants contained in (5) are  $B_{cr} = 10$ ,  $B_{me} = 100$ ,  $Ko = 10$ ,  $\underline{\omega} = 0.05$ ,  $\theta_0 = 0.83$ . The parameter p characterizing moisture transport was adopted equal to 0, 0.05, and 0.25. Figure 1 shows the distributions of the dimensionless total moisture  $\omega_S$  along the length of the specimen  $\xi$  at different instants, corresponding to  $p = 0.05$  (Fig. 1a) and  $p = 0.25$  (Fig. 1b). If there is no migration ( $p = 0$ ), the total moisture remains unchanged, i.e.,  $\omega_S = 1$ . In the former case (Fig. 1a) we find a maximum on the curve of total moisture in the frozen zone; this corresponds to the accumulation of moisture in the region adjacent to the freezing front. Here the moisture does not manage to migrate to the cold face, and it crystallizes, accumulating inside the frozen zone. In the latter case the coefficient p is five times as large as in the former case, and here we find a qualitatively different picture — the moisture migrates through the entire frozen zone and accumulates in the left side.

Figure 2 shows the distribution graphs of the function  $S = \omega - \omega_{of}(\theta)$  (7). It is characteristic that when there is no moisture transport (Fig. 2a), the region of nonequilibrium phenomena is situated chiefly at the freezing front. An increase of the parameter p, and consequently also of the moisture conductivity, has the effect that the nonequilibrium zone becomes more elongated (Fig. 2b), and with certain values of p it occupies the entire region of subzero temperatures (Fig. 2c). That means that during a fairly long time, the amount of nonfreezing water in the cold part of the sample differs considerably from its equilibrium value. Consequently, in this case the description of the moisture movement, based only on the equilibrium curve of nonfreezing water, is incorrect.

Moisture Distribution in Frozen Soils. In accordance with the remarks explained at the beginning of the present article, a simplified system (6) was used in solving the problems

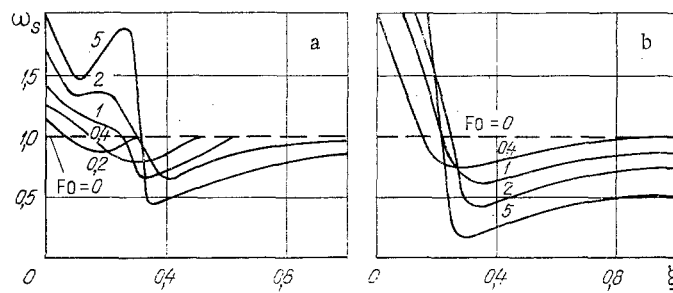


Fig. 1. Dynamics of the distribution of total moisture in one-sided freezing according to the data of numerical simulation with  $B_{cr} = 10$ : a)  $p = 0.05$ ; b)  $0.25$ .

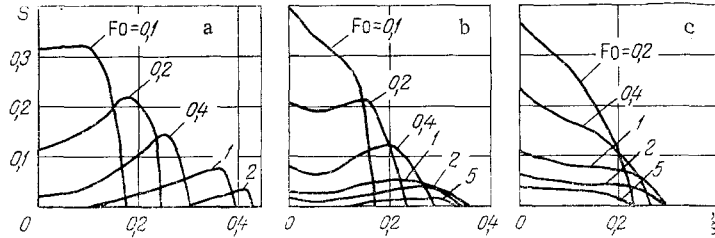


Fig. 2. Results of the numerical simulation of the distribution of the nonequilibrium function in one-sided freezing: a)  $p = 0$ ; b)  $0.05$ ; c)  $0.25$ .

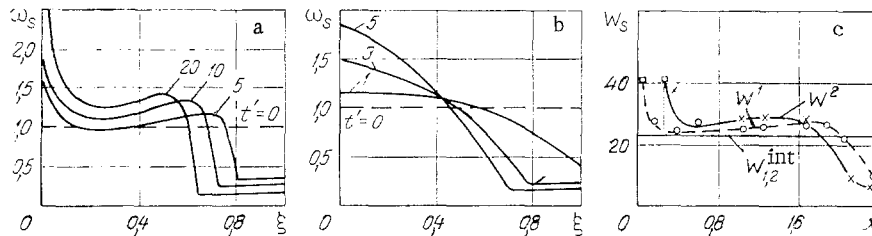


Fig. 3. Dynamics of the distribution of total moisture in a frozen sample of soil exposed to the effect of a constant temperature gradient: a)  $D_{cr} = 50$ ;  $D_{me} = 100$ ; b)  $D_{cr} = 5$ ;  $D_{me} = 10$  (results of simulation); c) experimental data.  $W_s$ , %;  $x$ , cm.

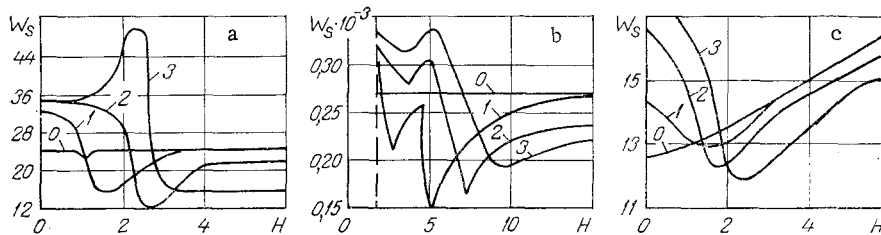


Fig. 4. Experimental data on the distribution of total moisture in one-sided freezing: 0) at the beginning of the experiment; 1, 2, 3) at subsequent instants.  $W_s \cdot 10^{-3}$ ,  $\text{kg}/\text{m}^3$ ;  $H$ , cm.

of moisture redistribution under the effect of a constant temperature gradient. The calculations were carried out for a soil whose nonfreezing water has an equilibrium curve similar to  $W_{of}(T)$  of Kiev clay. The dimensionless function of the nonfreezing water had the form  $\omega_{of}(\theta) = 0.205/(-\theta + 0.714)$ . The other constants assumed the following values:  $\theta_0 = 0.143$ ,  $\bar{\omega} = 0.5$ ,  $D_{cr} = 50$ ,  $D_{me} = 100$  (Fig. 3a);  $D_{cr} = 5$ ,  $D_{me} = 10$  (Fig. 3b). In the given problem the variants differ only in the parameters characterizing the kinetics of phase transitions. Figure 3a, b contains the distribution graphs of the total moisture  $\omega_s(\xi, t)$  with respect to  $t$  of the length of the sample  $\xi$  with different values of dimensionless time.

Figure 3a shows a variant corresponding to short crystallization and melting times. Here the total moisture assumes the largest value at the cold face and at the central part of the sample where the distribution has its maximum. An increase of the crystallization time  $\tau_{cr}$  and of the melting time  $\tau_{me}$  leads to a blurring of the maximum on the curve of total moisture. Beginning with some value of the constants, the maximum  $\omega_S$  vanishes, and the entire moisture migrates to the cold side without accumulating in the central part of the sample. However, it follows from Fig. 3a that even when the crystallization and melting times are short, the maximum on the curve of total moisture shifts toward temperature decrease, and eventually it can be seen that the entire moisture, like in Fig. 3a, moves to the colder side.

Discussion of Results. As noted before, the literature contains information on the nature of the water distribution during the freezing of wet soils. The distribution graphs of total moisture along the sample at different instants and for different soils, published in [1, 2], are shown in Fig. 4. The total moisture  $W_S$  was determined here according to the absorption of gamma rays. Figures 4a, b coincide qualitatively with the results of theoretical calculations (Fig. 1a). Figures 1b and 4c correspond to the freezing regime in which the moisture accumulates at the cold end. The experimental profiles of total moisture  $W_S$  during redistribution of moisture in frozen soil, obtained with the aid of twin samples [3], are shown in Fig. 3c. Here we may also speak of qualitative coincidence of the experimental data with the results of calculations (Fig. 3a).

It must be noted that in the notions on simulation discussed in the present article there was no place anywhere for the peculiarities of moisture migration when there are ice schlieren. This problem requires special investigation, because an ice interlayer closing off the migration paths of the moisture may cause a qualitative change of the nature of mass transfer. For instance, it is possible that the solid phase of water accumulates in the region of ice schlieren, as was observed in [3]. On the whole, a comparison of the results of numerical simulation of the process of freezing of moist soils with the experimental data available in the literature permits the conclusion that there is qualitative agreement between the simulation equations and the physical pattern.

#### NOTATION

$B$ , length of the sample, m;  $B_{cr} = cb^2/\lambda\tau_{cr}$ ;  $B_{me} = cb^2/\lambda\tau_{me}$ , dimensionless parameters;  $c$ , heat capacity of the soil,  $J/m^3 \cdot \text{deg}$ ;  $D_{cr} = b^2/W_0k\tau_{cr}$ ,  $D_{me} = b^2/W_0k\tau_{me}$ , dimensionless parameters;  $Fo = \lambda t/cb^2$ , Fourier numbers;  $h$ , space step;  $k$ , moisture conductivity,  $m^2/\text{sec}$ ;  $Ko = W_0\kappa/c|T_1|$ , Kossovich number;  $L$ , ice ratio, a.u.;  $\bar{L} = L/W_0$ , dimensionless ice ratio;  $p = W_0kc/\lambda$ , dimensionless parameter;  $q$ , migration flow of moisture, m/sec;  $S = \omega - \omega_{of}(\theta)$ , nonequilibrium function;  $T$ , soil temperature,  $^{\circ}C$ ;  $T_0$ , initial soil temperature,  $^{\circ}C$ ;  $T_1$ , temperature of the cold sample wall,  $^{\circ}C$ ;  $T_{of}(W)$ , temperature of incipient freezing of the soil,  $^{\circ}C$ ;  $t$ , time, sec;  $t' = kW_0t/b^2$ , dimensionless time of moisture migration;  $W$ , moisture, a.u.;  $W_0$ , initial moisture, a.u.;  $\underline{W}$ , minimum moisture below which moisture transport in the liquid phase ceases, a.u.;  $W_{of}(T)$ , curve of nonfreezing water, a.u.;  $W_S$ , total moisture, a.u.;  $\omega = W/W_0$ , dimensionless moisture;  $\underline{\omega} = W/W_0$ , dimensionless limiting moisture;  $\omega_{of}(\theta) = W_{of}(T)/\omega_0$ , dimensionless curve of nonfreezing water;  $\omega_i^n$ , dimensionless moisture calculated at the  $i$ -th node at the instant  $Fo = n\Delta Fo$ ;  $\Delta Fo$ , time step;  $\kappa$ , latent heat of the phase transition water-ice,  $J/m^3$ ;  $\lambda$ , thermal conductivity of the soil,  $W/m \cdot \text{deg}$ ;  $\sigma(T)$ , Heaviside function;  $\theta = T_0/|T_1|$ , dimensionless temperature;  $\theta_0 = T_0/|T_1|$ , dimensionless initial temperature;  $\theta_i^n$ , dimensionless temperature calculated at the  $i$ -th node at the instant  $Fo = n\Delta Fo$ ;  $\theta_{of}(\omega)$ , dimensionless temperature of incipient freezing of soil with moisture  $\omega$ ;  $\tau$ , relaxation time, sec;  $\tau_{cr}$ ,  $\tau_{me}$ , crystallization and melting time, respectively, sec;  $\xi = x/b$ , dimensionless space coordinate.

#### LITERATURE CITED

1. L. V. Chistotinov, Migration of Moisture in Freezing Water-Unsaturated Soils [in Russian], Nauka, Moscow (1973).
2. P. Hoekstra, "Moisture movement in soil under temperature gradients with the cold-side temperature below freezing," Water Resources Review, 2, No. 2, 241-250 (1966).
3. É. D. Ershov, Moisture Transport and Cryogenic Texture in Disperse Rocks [in Russian], Moscow State Univ. (1979).
4. V. Ya. Khain, "Depth of freezing of soil when there are migration and zones of phase transformations of the soil water," in: Cryogenic Processes, Nauka, Moscow (1978), pp. 156-169.

5. V. A. Kudryavtsev (ed.), General Geocryology [in Russian], Moscow State Univ. (1978).
6. Yu. S. Daniélyan and P. A. Yanitskii, "Kinetics of the freezing of water in moist soils," *Izv. Sib. Otd. Akad. Nauk. SSSR, Ser. Tekh. Nauk*, 3, No. 13, 89-92 (1979).
7. Yu. S. Daniélyan and P. A. Yanitskii, "Nonequilibrium effects in processes of freezing of moist soils," in: *Design of Equipment for the Oil Deposits of Western Siberia*, Tr. SibNIINP, No. 48, Tyumen' (1979), pp. 171-182.
8. G. A. Martynov, "Derivation of the principal equation of the heat conduction of freezing and thawing soils," in: *Materials on the Fundamentals of the Science of Permafrost Zones of the Earth's Crust*, Izd. Akad. Nauk SSSR, Moscow (1956), pp. 167-178.
9. A. N. Tikhonov and A. A. Samarskii, *Equations of Mathematical Physics* [in Russian], Nauka, Moscow (1972).

## CALCULATION AND DESIGN OF RADIATORS FOR THE AIR COOLING SYSTEM

### OF A GROUP OF INSTRUMENTS

O. B. Aga, G. N. Dul'nev,  
and B. V. Pol'shchikov

UDC 536.24

The article suggests a method of selecting the cooling regime and of planning the design of a radiator for a group of electronic instruments.

1. Thermal Model and Analysis of the Efficiency of the Radiators. Various radiators have found widespread application in electronics, radio engineering, electrical engineering, and other branches of instrument making for the purpose of cooling thermally loaded elements.

In design these devices differ according to the kind of developed surface [1]: lamellar, finned, pin type, "crab" type, louver type, and wire loop. The magnitude of the scattered power is substantially affected by the following geometric parameters: dimensions of the base ( $L_x$ ,  $L_y$  for rectangular radiators;  $D$  — the diameter — for circular radiators), height  $H$  and thickness  $d$  of the fin or pin, and pitch  $S$  between them. For wire-loop radiators we have to take into account the height of a turn  $H$ , the wire diameter  $d$ , the pitch of cooling  $S$ , the spacing of the coils  $S'$ , and the space factor of the channel  $\varphi$ , equal to the ratio of the cross-sectional area of the coils to the cross-sectional area of the channel. The values of the above parameters for the industrially produced radiators found expression in the corresponding standard and technical documentation [1-3].

For the individual cooling with natural or forced ventilation of low-power instruments, it is usual to use lamellar, finned, pin type, or "crab" type radiators. When the requirements as to the weight of the instrument are stringent, it is recommended to use pin type radiators; when the requirements concern mainly the size, finned radiators are recommended. Louver radiators with forced ventilation are used for cooling medium-power instruments; for groups of low- and medium-power instruments, single-group radiators are used, mostly finned or pin type radiators; they are economically and technologically more advantageous than individual radiators.

Investigation of the heat exchange of various types of radiators made it possible to plot the approximate dependence of the mean superheating  $\theta_s = t_s - t_c$  of the base with area  $S_p = L_x \cdot L_y$  on the specific load  $P/S_p$  with natural and forced ventilation (Fig. 1), from which it is then possible to choose the type of radiator and the nature of the heat exchange. The area bounded by the curves  $a_1-b_1$  pertain to a certain type of radiator with free or forced ventilation. For instance, the area  $a_1-b_1$  encompasses the values of  $P/S_p$  for different sizes of lamellar radiators with natural ventilation,  $a_4-b_4$  with forced ventilation, etc.

To characterize the heat exchange properties of radiators, the correlation between the mean superheating  $\theta_s$  of the base, the scattered power  $P$ , the effective heat transfer coefficient  $\alpha_{ef}$ , the thermal conductivity  $\sigma_\Sigma$ , and the thermal resistance  $R_\Sigma$  is often used:

---

Leningrad Institute of Precision Mechanics and Optics. Translated from *Inzhenerno-Fizicheskii Zhurnal*, Vol. 44, No. 1, pp. 99-105, January, 1983. Original article submitted September 29, 1981.